OPEN

PRS GLOBAL OPEN

ORIGINAL ARTICLE
Research

Keloidal Collagen May Be Produced Directly by αSMA-positive Cells: Morphological Analysis and Protein Shotgun Analysis

Chiemi Kaku, MD
Shizuko Ichinose, PhD
Teruyuki Dohi, MD, PhD
Mamiko Tosa, MD, PhD
Rei Ogawa, MD, PhD, FACS

Background: Keloids are fibroproliferative lesions caused by abnormal dermal wound healing. Keloidal collagen (KC) is a pathognomic feature of keloids, but the mechanism by which it forms is unknown. This study aimed to evaluate the histopathology of KC and thereby gain clues into how it forms.

Methods: The cross-sectional study cohort consisted of a convenience series of patients with keloids who underwent surgical excision. Skin pieces (3 mm^2) were collected from the keloid center and nearby control skin. Histopathology was conducted with light and electron microscopy and immunohistochemistry. KC composition was analyzed with protein shotgun analysis.

Results: Microscopic analyses revealed the ubiquitous close association between KC and αSMA-positive spindle-shaped cells that closely resembled myofibroblasts. Neither KC nor the spindle-shaped cells were observed in the control tissues. Compared with control skin, the collagen fibers in the KC were overall thinner, their diameter varied more, and their spacing was irregular. These features were particularly pronounced in the collagens in the vicinity of the spindle-shaped cells. Protein shotgun analysis did not reveal a specific collagen in KC but showed abnormally high abundance of collagens I, III, VI, XII, and XIV.

Conclusions: These findings suggest that KC may be produced directly by myofibroblasts rather than simply being denatured collagen fibers. Because collagens VI and XII associate with myofibroblast differentiation, and collagen XIV associates with local mechanical stress, these collagens may reflect, and perhaps contribute to, the keloid-specific local conditions that lead to the formation of KC.
(Plast Reconstr Surg Glob Open 2023; 11:e4897; doi: 10.1097/GOX.0000000000004897; Published online 10 April 2023.)

INTRODUCTION

Keloid is a fibroproliferative disorder of the skin that is caused by abnormal wound healing in the dermis after cutaneous inflammation and injury.[1,2] The pathognomic histopathological features of keloids are keloidal collagen (KC), which is haphazardly arranged, and abundant whorls of thickened hyalinized collagen bundles that interconnect and thereby generate a thick layer in the reticular dermis.[3] At present, it is not clear how KC develops.[3–5] Our previous histological study[6] showed that very young keloids (ie, lesions 3 months after onset) already bear some KC. Moreover, the keloid area that is occupied by KC increases significantly over time ($P < 0.05$). Thus, KC production in keloids seems to begin soon after onset and increases over time, and the KC does not spontaneously disappear. This led us to speculate that KC may be actively produced by specific cell types rather than by passive collagen fiber degeneration.

In the present study, we considered this KC-producing cell as a potential target for keloid therapy and comprehensively analyzed KC histopathology in multiple keloids by light microscopy, transmission electron microscopy (TEM), and immunohistochemistry. We also used protein shotgun analysis to identify the molecular components of KCs.

From the Department of Plastic, Reconstructive and Aesthetic Surgery, Nippon Medical School, Tokyo, Japan.

Received for publication November 30, 2022; accepted February 6, 2023.

Copyright © 2023 The Authors. Published by Wolters Kluwer Health, Inc. on behalf of The American Society of Plastic Surgeons. This is an open-access article distributed under the terms of the Creative Commons Attribution-Non Commercial-No Derivatives License 4.0 (CCBY-NC-ND), where it is permissible to download and share the work provided it is properly cited. The work cannot be changed in any way or used commercially without permission from the journal.

DOI: 10.1097/GOX.0000000000004897

Disclosure: The authors have no financial interest to declare in relation to the content of this article.

Related Digital Media are available in the full-text version of the article on www.PRSGlobalOpen.com.

MATERIALS AND METHODS

Study Design and Ethics

This prospective cross-sectional study was conducted according to the tenets of the Helsinki Declaration and was approved by the ethics committee of Nippon Medical School Hospital, Tokyo, Japan (Ethics Approval No.: 29-05-760). All patients provided written consent to participate in the study.

Patient Recruitment

The study cohort was a convenience series of Japanese patients who underwent resection of a keloid (n = 16). The age, sex, keloid site, cause, and time since the onset of disease for the 16 patients who met study eligibility criteria are listed in Table 1; cases 1–13 underwent morphological and immunohistochemical analysis using light and electron microscopy, and cases 14–16 underwent protein shotgun analysis. The inclusion and exclusion criteria used to select patients are detailed in Table 2. The morphological and protein shotgun patients were recruited in separate studies.

Surgery, Tissue Collection, Processing, and Study Plan

In each surgery, the keloid was excised with minimal margins. Moreover, to control for age, sex, body site, and other differences between the morphological-analysis patients, healthy skin samples were obtained during surgery. These samples were the skin tags that were generated during suturing. All were located 5–15 mm from the keloid margin. A scalpel was used to cut 3-mm^2 pieces of skin from both the keloid center and the control skin samples. An example is shown in Figure 1.

Table 1. Demographic and Clinical Characteristics of the Patients

Case	Age/ Gender	Sites	Cause	The Duration of Illness	Diagnosis
1	46/M	Chest	Acne	30 y	Keloid
2	64/M	Chest	Acne	17 y	Keloid
3	25/M	Chest	Insect bite	12 y	Keloid
4	26/M	Shoulder/ upper arm	Surgery/ vaccination	unknown	Keloid
5	11/M	Chest/thigh	Surgery/peel off-wound	1 y	Keloid
6	5/F	Buttock	Peel off-wound	1 y	Keloid
7	68/M	Chest	Epidermal cyst	10 y	Keloid
8	58/M	Chest/navel	Surgery	2 y	Keloid
9	36/F	Abdomen	Surgery	5 y	Keloid
10	73/M	Chest	Acne	over 30 y	Keloid
11	50/M	Neck	Surgery	17 y	Keloid
12	36/M	Chest/lower jaw	Acne	8 y	Keloid
13	49/M	Chest	Acne	29 y	Keloid
14	20/F	Earlobe	Piercing	10 mo	Keloid
15	13/M	Earlobe	Trauma	6 mo	Keloid
16	20/F	Earlobe	Piercing	2 y	Keloid

M, masculine; F, feminine.

Takeaways

Question: This study aimed to evaluate the histopathology of keloidal collagen (KC) and thereby gain clues into how it forms.

Findings: Skin pieces were collected from the keloid center and nearby control skin. Histopathology conducted with light and electron microscopy and immunohistochemistry revealed the ubiquitous close association between KC and αSMA-positive spindle-shaped cells that closely resembled myofibroblasts. Compared with control skin, the collagen fibers in the KC were overall thinner, their diameter varied more, and their spacing was irregular.

Meaning: These findings suggest that KC may be produced directly by αSMA-positive spindle-shaped cells rather than simply being denatured collagen fibers.

Table 2. Inclusion and Exclusion Criteria Used to Recruit Patients for the Study

The Inclusion Criteria	The Exclusion Criteria*
(i) Clinical diagnosis of keloid by an experienced clinician on the basis of the typical keloid shape, growth beyond the wound margin, elevation, induration, and redness. (ii) The diagnosis led to the decision between the patient and the clinician that the lesion(s) would be resected surgically. (iii) The patient underwent the surgery as planned. (iv) The extirpated lesion was subjected to pathology by an experienced pathologist.	(i) Postoperative histological diagnoses other than keloids. (ii) Preoperative presence of other skin diseases, underlying diseases such as hypertension or diabetes mellitus, and patients taking anticoagulants or immunosuppressive drugs.

*These conditions can cause morphological abnormalities in the skin.

Light Microscopy

The tissue specimens were fixed for 2 hours with 2.5% glutaraldehyde in 0.1 M phosphate-buffer (PB), post-fixed with 1% osmium tetroxide buffered with 0.1 M PB for 2 hours, dehydrated with a graded series of ethanol, embedded in Epon 812, and sliced into semi-thin (thickness: 1 μm) sections. The sections were laid on glass slides and stained for 30 seconds with toluidine blue. Alternatively, to identify the eosin-staining hyalinized area, the Epon was removed with a mixed solution of NaOH and xylene, and the slides were washed with water and stained, first with toluidine blue and then with eosin. Light microscopy (BZ-9000, KEYENCE, Osaka, Japan) was then conducted.

Transmission Electron Microscopy

Some of the sections obtained for light microscopy were thinned further into ultrathin sections (thickness: 80–90 nm), placed on copper grids, double-stained with

Fig. 1. Collection of keloid tissues. A representative keloid that was excised by surgery is shown. The 3-mm^2 pieces of skin that were collected from the center of the keloid (a) and the control skin near the keloid (b) are shown.

uranyl acetate and lead citrate, and then examined with a transmission electron microscope (JEM-1400plus, JEOL, Tokyo, Japan). The short diameters of the collagen fibers in the KC center and the control tissue (300 locations/sample) were measured by photographing horizontal cross-sectional TEM images of the collagen fibrils and then using Image J (Vienna, Austria).

Immunohistochemistry

The tissue specimens were fixed for 1 hour with 4% paraformaldehyde in 0.1 M PB, mounted in OCT compound (Sakura Finetek Japan Co., Ltd., Tokyo, Japan), and quickly frozen in liquid nitrogen. Frozen sections were cut on a Tissue-Tek (Sakura Finetek Japan Co., Ltd., Tokyo, Japan) at a temperature of -15°C, placed on silane-coated glass slides. The slides were immunostained with horse anti-mouse α-smooth muscle actin antibody (Sigma-Aldrich, Ca.) by using the Vectastain ABC kit (Vector Laboratories, Burlingame, Ca.). Briefly, the sections were blocked with 0.3% H_2O_2 for 5 minutes and diluted with normal blocking serum for 20 minutes and then incubated with anti-α-smooth muscle actin antibodies (diluted to 1:200 in 0.1 M PB) in 5% bovine serum albumin for 30 minutes. After washing with PB saline, the sections were incubated for 30 minutes with biotinylated secondary antibody. After washing, TaKaRa DAB Substrate (TAKARA BIO INC., Shiga, Japan) was added. Nuclear counterstaining was performed with Mayer's hematoxylin. Light microscopy was then conducted (BZ-9000, KEYENCE, Osaka, Japan).

Protein Shotgun Analysis

The central keloid pieces were fixed with formalin and embedded in paraffin. The KC therein was then excised using the microdissection method and incubated at 95°C for 1 h and then at 60°C for 2 hours in lysis buffer that included 100 mM ammonium bicarbonate and 20% acetonitrile. After sonication for 10 minutes using Bioruptor UCD-250 (Sonicbio Co., Ltd., Kanagawa, Japan), the samples were reduced by adding dithiothreitol to a final concentration of 134 mM and then incubating the mixture for 5 minutes at 95°C. The free thiol groups were alkylated with 230 mM iodoacetamide at room temperature for 30 minutes in the dark. Finally, the samples were digested with Trypsin (APRO Science Co., Ltd., Tokyo, Japan) overnight at 37°C.

LC-MS/MS protein analysis was then conducted.[7] Thus, the peptides in the digested samples were prepared for mass spectrometry analysis by using GL-Tip strong cation exchange chromatography (GL Science Inc., Tokyo, Japan). Thus, the samples were reconstituted in the starting buffer [10 mM KH_2PO_4 (pH 3)/25% acetonitril/10 mM KCl], after which the peptides were eluted off with the elution buffer [10 mM KH_2PO_4 (pH 3)/25% acetonitril/350 mM KCl]. Each elution was concentrated by vacuum centrifugation and resuspended in 50 µL 0.1% (v/v) formic acid. The samples were desalted with SPE C-Tip (Nikkyo Technos, Co., Ltd., Tokyo, Japan), concentrated again by vacuum centrifugation, and resuspended in 40 µL 0.1% (v/v) formic acid. All samples were stored at -20°C until LC-MS analysis.

MS/MS spectra were acquired from the recovered peptides by using Q Exactive Plus (Thermo Fisher Scientific Inc., Tokyo, Japan) coupled online with a capillary high-performance liquid chromatography system (EASY-nLC 1200; Thermo Fisher Scientific Inc., Tokyo, Japan). A 0.075×150 mm-EASY-Spray column (3-µm particle diameter, 100 Å pore size, Thermo Fisher Scientific) with 0.1% formic acid and 0.1% formic acid/80% acetonitrile mobile phases was used. The data derived from the MS/MS spectra were used to search the SWISS-Prot protein database by using the MASCOT Server (http://www.matrixscience.com) and identify proteins by using the program Scaffold viewer (http://www.proteomesoftware.com/products/scaffold).

Statistics

The demographic and clinical variables were expressed as mean (range) or n (%). Collagen fiber diameters were assessed for normality by the Shapiro-Wilk test, and the data were expressed as median and interquartile range. KC and control samples were compared in terms of collagen fiber diameter by using the Mann-Whitney *U* test. Power analyses were not conducted due to the descriptive nature of this study. Differences were considered statistically significant at *P* less than 0.05. All statistical analyses were performed with EZR (Saitama Medical Center, Jichi Medical University; Http://www.jichi.ac.jp/saitama-sct/SaitamaHP.files/statmedEN.html; Kanda, 2012), which is a graphical user interface for R (The R Foundation for Statistical Computing, Vienna, Austria).

RESULTS

Patients Participating in the Morphological Analyses

The 13 keloids were subjected to light microscopic, TEM, and immunostaining analyses. The characteristics of these 13 patients are shown in Table 1 (cases 1–13).

Light Microscopy Observation of KC

Cross-sectional light microscopy of the toluidine blue- and eosin-stained central part of the keloids showed the presence of both a fibrous component that stained red with eosin and a cellular component that stained blue. In the reticular layer of the dermis, the fibrous material formed very thick fibers that were strongly dyed with eosin and ran in a complicated manner (Fig. 2). This material was considered to be KC. Semi-subjective quantification showed that KC was never found in the control adjacent skin samples (Table 3). Toluidine blue staining alone showed that the KC was interspersed with new blood vessels and infiltrating cells, including mast cells (Fig. 3). The papillary layer of the dermis contained many more cellular components and new blood vessels but no KC (Fig. 2).

TEM and Immunohistochemistry Observations of KC

Low-magnification TEM images showed that the collagen aggregates were surrounded by cells (endothelial cells, erythrocytes, platelets, blood cells, and mast cells) and many new blood vessels with two to three layers of vascular structure. In many cases, the lumen seemed to be obstructed or narrowed. Sometimes the vascular structure was disrupted and there were findings suggesting leakage of cellular components such as red blood cells and platelets. Cell fragments were found around the new blood vessels. The blood vessels were surrounded by intricate collagen fibers (Fig. 4A).

Higher-magnification TEM images showed that the KC was inevitably accompanied by spindle-shaped cells. These cells showed prominent rough endoplasmic reticulum, peripheral myofilaments, fibronectin filaments, reticular collagen fibers, dense bodies near the cell wall, and fibronexus junctions.[8,9] These cells seemed to be producing collagen (Fig. 4B–D). Immunostaining of these cells for αSMA showed that all were positive for this marker (Fig. 5).

In the TEM images, the collagen fibrils at the center of the KC region were thinner, had a more complex fibril orientation, and seemed to be partially fused compared with the collagen fibrils in the control skin near the keloid (Fig. 6). Therefore, we measured and analyzed the

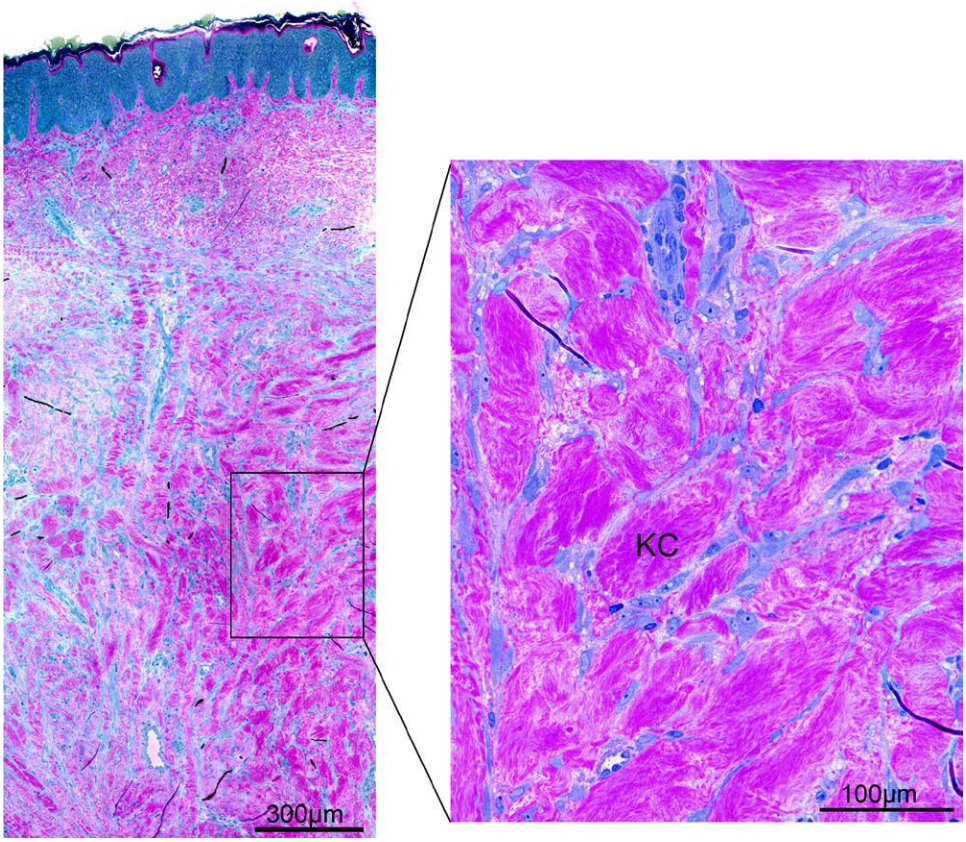

Fig. 2. Light microscopy image of toluidine blue– and eosin-stained keloid tissue in cross-section. A representative image of the 13 keloid pieces is shown in cross-section. The KC is the red streak–like hyalinized areas in the reticular layer of the dermis.

Table 3. Amount of KC in the Toluidine Blue– and Eosin-stained Keloid and Control Skin Tissues

Case	1	2	3	4	5	6	7	8	9	10	11	12	13
Control skin	–	–	–	–	–	–	–	–	–	–	–	–	–
Keloid center*	+	+	++	++	+	++	++	+++	+++	++	+++	+	++

*The amount of KC was quantified semi-subjectively as none (–), little but present (+), moderate (++), and abundant (+++).

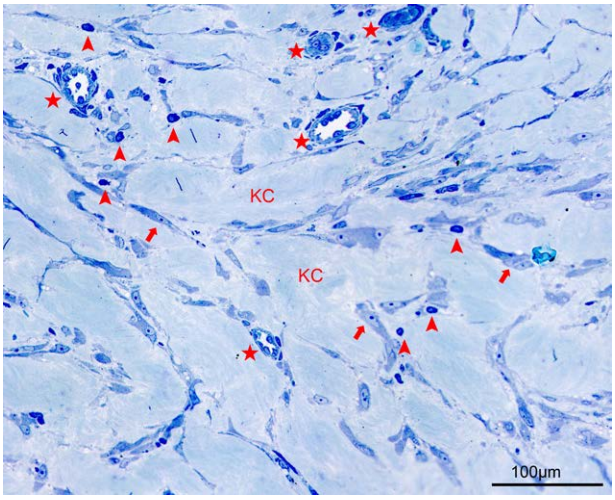

Fig. 3. Light microscopy image of toluidine blue–stained keloid tissue in cross-section. A representative image of the keloid pieces is shown in cross-section at 100-μm magnification. The KC in the reticular dermis is interspersed with new blood vessels (★) and infiltrating cells (↑), including mast cells (▲).

diameter of 300 collagen fibers in KC and control skin from TEM images of three samples, which were randomly selected from the 13 morphologically analyzed samples. Only three keloids were subjected to these analyses due to the obvious differences between KCs and controls that were observed. The results showed that the collagen fibers at the KC center were significantly thinner than the collagen fibers in control skin (all $P < 0.0001$) (Fig. 7). (**See table, Supplemental Digital Content 1**, which displays collagen fibril diameters in the central KC area and control skin of three patients, as determined by measuring 300 fibers/sample in TEM images. **http://links.lww.com/PRSGO/C469**.)

Protein Shotgun Analysis

For protein shotgun analysis, three keloid samples were collected from patients who did not participate in the morphological analyses. The characteristics of these three patients are shown in Table 1 (cases 14–16). Protein shotgun analysis of the KC in each sample identified 500, 621, and 552 proteins, respectively. Of the 371 proteins that these samples shared, 306 were extracellular matrix

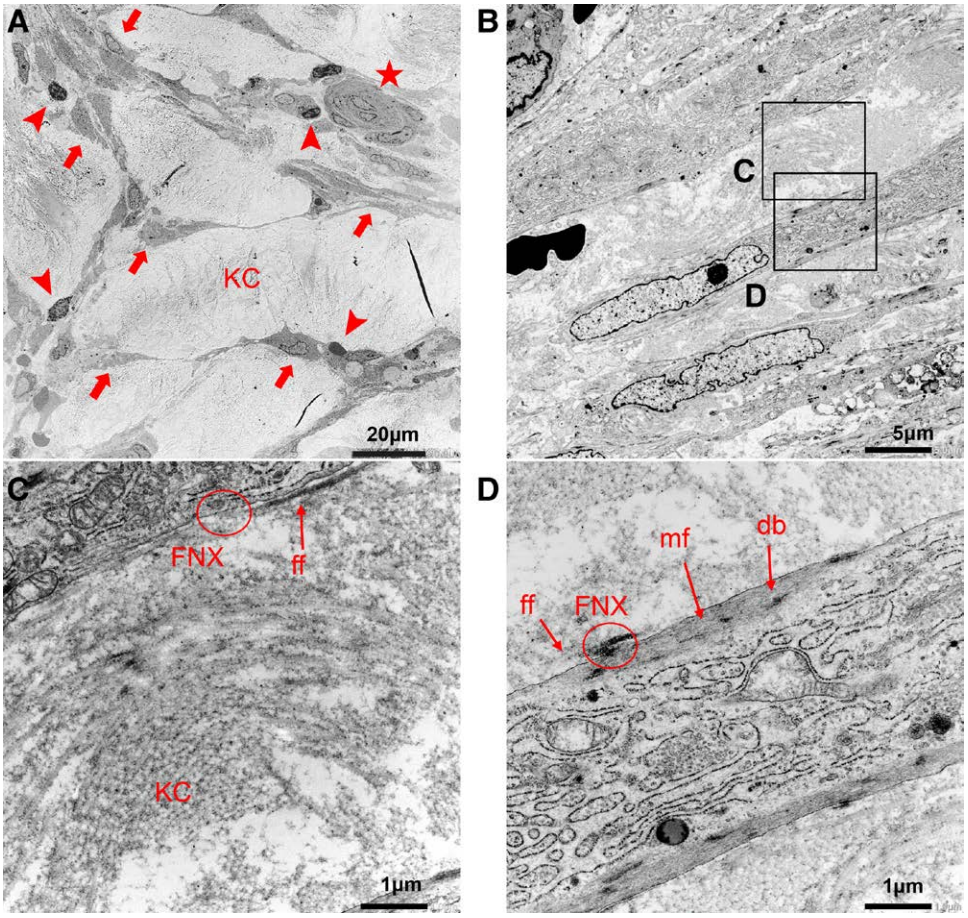

Fig. 4. TEM images of keloid tissue. A representative image of the keloid pieces is shown in cross-section at 20-μm (A), 5-μm (B), and 1-μm (C and D) magnification. In A, the KC is marked by KC, the blood vessels by ★, and the infiltrating cells by ↑. The mast cells are indicated by ▲. The image in B is a magnification of the area near the cells in A. The areas in B that are magnified in C and D are indicated by the inset borders. Spindle-shaped cells can be seen. In C and D, KC is indicated by KC, fibronexus by FNX, fibronectin filaments by ff, myofilaments by mf, and dense body by db.

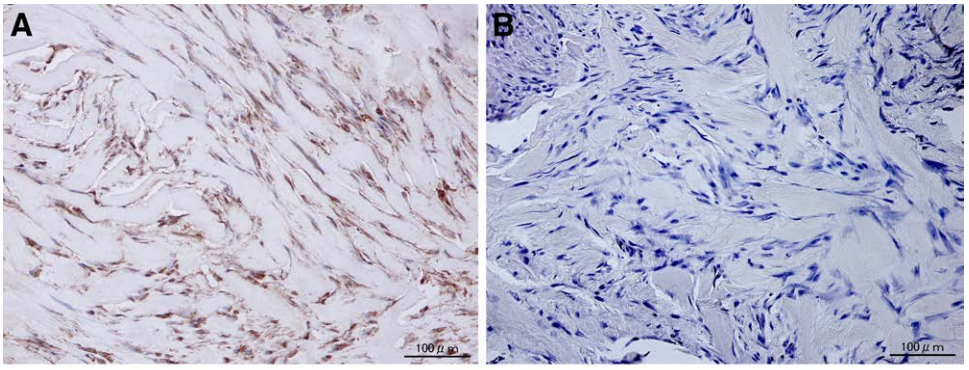

Fig. 5. Immunohistochemistry image of αSMA expression in the KC area. A representative of the keloid pieces that underwent immunohistochemistry for αSMA expression is shown in cross-section at 50-μm magnification. A, Immunostaining for αSMA. B, The negative control lacking the anti-αSMA antibody.

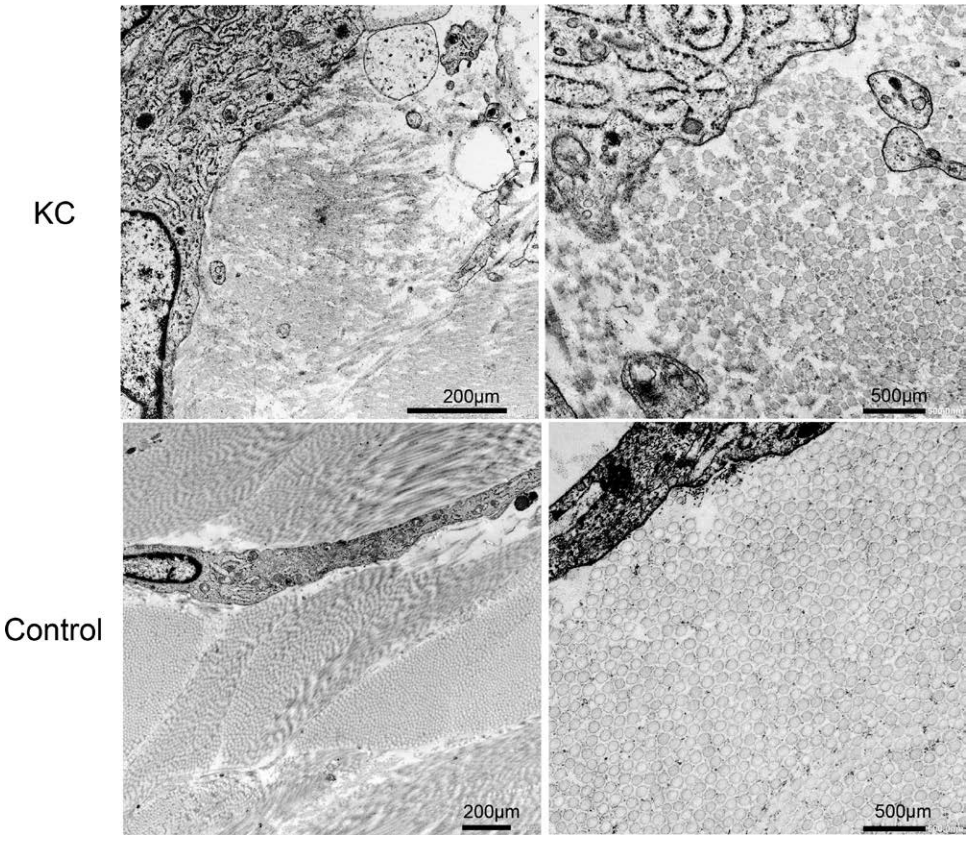

Fig. 6. TEM images of the collagen fibers in the KC area. Cross-section images are shown to the left, and longitudinal section images are shown to the right. Upper panels: Collagen fibrils around the cells in the KC area. Lower panels: Collagen fibrils in the control skin.

components. The iBAQ values of these proteins were calculated. Only the 10 most abundant collagen components were reported in this study. Collagen type I (COL1A2 and COL1A1) was the most common component in KC. The KCs also expressed abundant amounts of collagen type III (COL3A1), XIV (COL14A1), VI (COL6A1–3), and XII (COL12A1). Unique collagen components were not found in the KC (Fig. 8).

DISCUSSION

The present study comprehensively analyzed KC in terms of its location, relationship to blood vessels and nearby cells, and molecular composition in multiple patients. We focused on KC because, in our experience, the only histological characteristic that truly defines keloids is KC in the reticular dermis. Others have suggested that keloids are also characterized by other histological

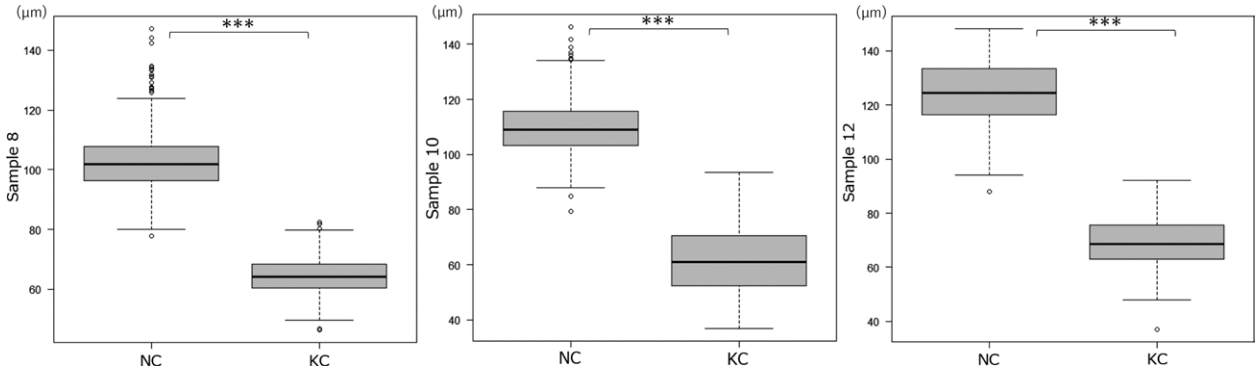

Fig. 7. Box plot showing comparison of collagen fibril diameters in the central KC area and control skin. The box line is the median, and the IQR is the difference between the third and first quartile. (***$P < 0.001$ by Mann-Whitney *U* test.).

Gene names	iBAQ	log(iBAQ)
COL1A2	9.51E+08	8.978372
COL1A1	6.89E+08	8.83832
COL3A1	2.32E+08	8.366404
COL14A1	1.08E+08	8.035069
COL6A3	92712000	7.967136
COL6A1	82899000	7.918549
COL12A1	47896000	7.680299
COL6A2	43007000	7.633539
COL5A1	2635100	6.420797
COL5A2	2611000	6.416807

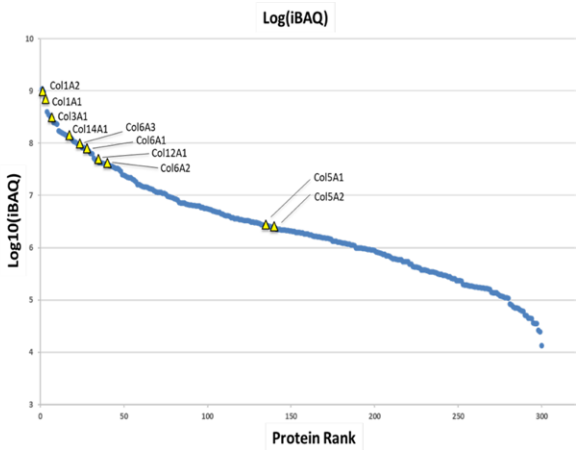

Fig. 8. Shotgun protein analysis of KC. The KCs of three keloids were microdissected and subjected to protein shotgun analysis followed by comparative quantification of the identified proteins by iBAQ values. The three keloid samples contained 500, 621, and 552 factors. They shared 371 factors. The 10 most abundant collagen factors are shown in the table. The relative abundances (log iBAQ) of the ten collagen factors were plotted.

features, namely, a thickened and flattened epidermis, keratin proliferation, infiltration of inflammatory cells in the papillary dermis, enlargement of the papillary dermis that obscures the boundary between the papillary dermis and the reticular layer, and a hyalinized complexion.[10] However, we find that the epidermal and papillary dermal features are not always observed. Moreover, hyalinization (vitrification), which refers to fusion of the collagen fibers that causes them to dye homogeneously in positive acidity, is reported not only in keloids[1,3,11,12] but also in scleroderma,[13] calcifying fibrous tumor,[14–17] carcinoma,[18] and sarcoma.[19–22] By contrast, KC has such unique features compared with the collagens in other disease histologies that dermatopathologists recognize it immediately.

Our study showed that compared with the collagen fibrils in nearby control skin, the collagen fibrils in the KC region were generally thinner, irregularly shaped, and unevenly spaced when viewed in cross-section. Furthermore, the orientation of the fibrils was complex, and multiple fusions were observed. These collagen fibrils are clearly different from the collagen fibrils produced by the indigenous fibroblasts of the control dermis. Notably, these abnormalities were also present in the collagen fibrils in the vicinity of the spindle-shaped cells that were always observed to lie adjacent to the KC bundles (Fig. 6). These findings suggest that the spindle-shaped cells generate collagen fibrils with different diameters, which then fuse together and accumulate as KC. This suggests that KC is produced by cells rather than by collagen denaturation. This is supported by our previous observation that KC is also present in young keloids and that it accumulates over time.[6]

The spindle-shaped cells that seemed to produce KC seemed to be myofibroblasts because they bore prominent rough endoplasmic reticulum, peripheral myofilaments, fibronectin filaments, reticular collagen fibers, dense bodies near the cell wall, abundant pericellular matrix, and fibronexus junctions.[8,23] The latter are cell-surface specializations consisting of intracellular actin filaments and extracellular fibronectin filaments that intimately connect the myofibroblast to the extracellular matrix; they are very characteristic of these cells.[9] Myofibroblasts are highly contractile cells that produce much more extracellular matrix than normal fibroblasts and have been closely linked to multiple fibrotic

diseases, including in the skin, heart, liver, lung, and kidney. They are generated by the mesenchymal transformation of various cell types, including resident fibroblasts, pericytes, vascular endothelial cells, smooth muscle cells, and macrophages. Although it remains unclear how these cells differentiate into myofibroblasts,[8,23] in vitro experiments have shown that healthy skin fibroblasts can differentiate into contractile collagen-overproducing myofibroblasts when they are exposed to inflammation that generates TGF-β1 or IL-6.[24,25] The possibility that the culprit KC-producing cells in keloids are myofibroblasts is supported by their ubiquitous location next to the KC bundles. This notion is also suggested by the hyalinization of KC, as observed by eosin staining and light microscopy: it is known that the collagen produced by myofibroblasts associates with fiber vitrification because myofibroblastoma (ie, benign myofibroblastic neoplasm) also produces hyalinized collagen.[26–29] In addition, our immunohistochemical analyses showed that the spindle-shaped cells bore αSMA, which is a widely used marker of myofibroblasts.[30] It should be noted that several recent studies have shown that αSMA is not always a consistent marker of the profibrotic contractile and collagen-producing functions of myofibroblasts in various fibrotic diseases,[31–33] including keloids.[34] Nonetheless, it is a relatively standard feature of myofiblasts.

It should be noted that due to convenience, the control skin samples were from skin tags and thus were all located 5–15 mm from the leading edge of the keloids. There is some evidence that such nearby skin differs from healthy skin further away from the keloid in terms of blood flow, lymphocytic infiltration, gene expression, and collagen fibers: in particular, the collagen fibers in skin near keloids tend to be thinner and more loosely organized than in skin further away.[35] This is likely to reflect various factors leaching from the keloid into the surrounding skin.[35] Nonetheless, the control skin samples in our study did not evince any KC and exhibited marked differences in collagen fiber morphology and organization, which supports their use as control samples. However, further studies should seek to use control skin samples that are situated further away from the inflamed keloid edge to limit bystander inflammatory effects.

Our protein shotgun analysis showed that KC is largely composed of collagen I, III, VI, XII, and XIV. Other studies have also reported that keloid associates with high collagen I and lower collagen III and, thus, has a high collagen I:III ratio.[36–40] The high levels of collagen XIV in KC are notable because this collagen is known to be upregulated in areas of high mechanical stress.[41] Local mechanical stress on the wound/scar is thought to be an important risk factor for the development and progression of keloids.[42] The abnormal abundance of collagen VI in keloids has been observed previously.[43] Collagen VI has multiple functions that link it to myofibroblast activity: specifically, it is a structural protein that binds a fibrosis-regulating hormone called endotrophin,[44] can promote myofibroblast differentiation,[45] and may prevent fibroblast apoptosis.[46,47] Significantly, collagen XII, which we observed is also present at high levels in KCs, is known to be a marker of myofibroblasts.[48] Further studies on the roles that collagen VI, XII, and XIV (and the other upregulated proteins that we detected by shotgun analysis) play in keloid pathogenesis and KC development are warranted.

It should be noted that the three samples we used for our shotgun analysis came from earlobe keloids, whereas the samples used for the microscopy studies were mainly from the torso. However, given that keloids share the same general histological features regardless of body site, we expect that our shotgun study findings will be recapitulated in keloids from other body sites. Nonetheless, further studies with torso keloids and higher sample sizes are warranted.

To date, attempts to produce KC in vitro or in animal models have failed.[49] This has greatly hindered our understanding of the mechanisms by which KC is created and whether/how KC contributes to the progression and treatment-refractoriness of keloids. Our study is useful in this regard because it suggests strongly that KC is produced by myofibroblasts and is not just denatured collagen fibers. Further in vitro research comparing keloid myofibroblasts, myofibroblasts in other diseases (which do not produce KC), and normal fibroblasts may help elucidate how these myofibroblasts produce KC and whether/how KC and its individual components contribute to the deranged cellular communications and signaling pathways that characterize keloids.[50] Such research could potentially elucidate therapeutic targets that could help prevent or ameliorate keloidal growth.

CONCLUSIONS

Little is known about the processes that produce KC. To our knowledge, this is the first time a study has asked whether KC is produced by local cells rather than by degeneration. Indeed, we observed that KC is morphologically distinct from control collagen fibers and appears to be produced directly by myofibroblast-like αSMA-positive cells. This suggests that KC adopts its unique features before and/or soon after it is secreted by local cells rather than being a degradation product.

Rei Ogawa, MD, PhD, FACS
Department of Plastic, Reconstructive and Aesthetic Surgery
Nippon Medical School
1-1-5 Sendagi Bunkyo-ku
Tokyo 113-8603, Japan
E-Mail: r.ogawa@nms.ac.jp

REFERENCES

1. Ogawa R. Keloid and hypertrophic scars are the result of chronic inflammation in the reticular dermis. *Int J Mol Sci* . 2017;18:606.
2. Ogawa R, Dohi T, Tosa M, et al. The latest strategy for keloid and hypertrophic scar prevention and treatment: the Nippon Medical School (NMS) protocol. *J Nippon Med Sch.* 2021;88:2–9.
3. Limandjaja GC, Niessen FB, Scheper RJ, et al. The keloid disorder: heterogeneity, histopathology, mechanisms and models. *Front Cell Dev Biol.* 2020;8:360.
4. Huang C, Ogawa R. The link between hypertension and pathological scarring: does hypertension cause or promote keloid and hypertrophic scar pathogenesis? *Wound Repair Regen.* 2014;22:462–466.
5. Limandjaja GC, Niessen FB, Scheper RJ, et al. Hypertrophic scars and keloids: overview of the evidence and practical guide

for differentiating between these abnormal scars. *Exp Dermatol.* 2021;30:146–161.
6. Matsumoto N, Peng WX, Aoki M, et al. Histological analysis of hyalinised keloidal collagen formation in earlobe keloids over time: collagen hyalinisation starts in the perivascular area. *Int Wound J.* 2017;14:1088–1093.
7. Vogeser M, Parhofer KG. Liquid chromatography tandem-mass spectrometry (LC-MS/MS)—technique and applications in endocrinology. *Exp Clin Endocrinol Diabetes.* 2007;115:559–570.
8. Eyden B. The myofibroblast: phenotypic characterization as a prerequisite to understanding its functions in translational medicine. *J Cell Mol Med.* 2008;12:22–37.
9. Eyden BP. Brief review of the fibronexus and its significance for myofibroblastic differentiation and tumor diagnosis. *Ultrastruct Pathol.* 1993;17:611–622.
10. Jumper N, Paus R, Bayat A. Functional histopathology of keloid disease. *Histol Histopathol.* 2015;30:1033–1057.
11. Lee JY, Yang CC, Chao SC, et al. Histopathological differential diagnosis of keloid and hypertrophic scar. *Am J Dermatopathol.* 2004;26:379–384.
12. Huang C, Murphy GF, Akaishi S, et al. Keloids and hypertrophic scars: update and future directions. *Plast Reconstr Surg Glob Open.* 2013;1:e25.
13. Kissin EY, Merkel PA, Lafyatis R. Myofibroblasts and hyalinized collagen as markers of skin disease in systemic sclerosis. *Arthritis Rheum.* 2006;54:3655–3660.
14. Fetsch JF, Montgomery EA, Meis JM. Calcifying fibrous pseudotumor. *Am J Surg Pathol.* 1993;17:502–508.
15. Van Dorpe J, Ectors N, Geboes K, et al. Is calcifying fibrous pseudotumor a late sclerosing stage of inflammatory myofibroblastic tumor? *Am J Surg Pathol.* 1999;23:329–335.
16. Hill KA, Gonzalez-Crussi F, Chou PM. Calcifying fibrous pseudotumor versus inflammatory myofibroblastic tumor: a histological and immunohistochemical comparison. *Mod Pathol.* 2001;14:784–790.
17. Shinohara N, Nagano S, Yokouchi M, et al. Bilobular calcifying fibrous pseudotumor in soleus muscle: a case report. *J Med Case Rep.* 2011;5:487.
18. Wood A, Young F, Morrison J, et al. Sclerosing odontogenic carcinoma presenting on the hard palate of a 43-year-old female: a case report. *Oral Surg Oral Med Oral Pathol Oral Radiol.* 2016;122:e204–e208.
19. O'Sullivan MJ, Sirgi KE, Dehner LP. Low-grade fibrosarcoma (hyalinizing spindle cell tumor with giant rosettes) with pulmonary metastases at presentation: case report and review of the literature. *Int J Surg Pathol.* 2002;10:211–216.
20. Kitagawa Y, Ito H, Sawaizumi T, et al. Fine needle aspiration cytology of primary epithelioid sarcoma. A report of 2 cases. *Acta Cytol.* 2004;48:391–396.
21. Kusumi T, Nishikawa S, Tanaka M, et al. Low-grade fibromyxoid sarcoma arising in the big toe. *Pathol Int.* 2005;55:802–806.
22. Thomison J, McCarter M, McClain D, et al. Hyalinized collagen in a dermatofibrosarcoma protuberans after treatment with imatinib mesylate. *J Cutan Pathol.* 2008;35:1003–1006.
23. Schürch W, Seemayer TA, Gabbiani G. The myofibroblast: a quarter century after its discovery. *Am J Surg Pathol.* 1998;22:141–147.
24. Vincent S, Fabrice B, Ludovic M, et al. Mechanisms of pathological scarring: role of myofibroblasts and current developments. *Wound Repair Regen.* 2011;19:s10–s15.
25. Shi LL, Zhang RF, Xiao H. Roles of interleukin-6/signal transduction and activator of transcription 3 pathway and β-catenin in mechanical stress-induced hypertrophic scar formation in mice. *Zhonghua Shao Shang Za Zhi.* 2021;37:647–653.
26. Calonje E, Fletcher CD. Aneurysmal benign fibrous histiocytoma: clinicopathological analysis of 40 cases of a tumour frequently misdiagnosed as a vascular neoplasm. *Histopathology.* 1995;26:323–331.
27. Kobayashi N, Oda K, Yokoi S, et al. Myofibroblastoma of the breast: report of a case. *Surg Today.* 1996;26:727–729.
28. Yusuf Y, Prasad ML, Osborne MP. Myofibroblastoma in the irradiated breast. *Breast J.* 1999;5:136–140.
29. Ning H, Jinyong L, Xuehan Q, et al. Intraocular myofibroblastoma in an infant: a case report. *BMC Ophthalmol.* 2015 Aug 25; 15:113.
30. Younesi FS, Son DO, Firmino J, et al. Myofibroblast markers and microscopy detection methods in cell culture and histology. *Methods Mol Biol.* 2021;2299:17–47.
31. Osama A, El-Mahdy A, Rizk S, et al. Alpha-smooth muscle actin (αSMA) gene, a possible derive of myofibroblasts in bone marrow fibrosis. *BMFJ.* 2020;37:439–448.
32. Zhao W, Wang X, Sun K, et al. α-smooth muscle actin is not a marker of fibrogenic cell activity in skeletal muscle fibrosis. *PLoS One.* 2018;13:e0191031.
33. Sun K, Chang Y, Reed NI, et al. α-Smooth muscle actin is an inconsistent marker of fibroblasts responsible for force-dependent TGFβ activation or collagen production across multiple models of organ fibrosis. *Am J Physiol Lung Cell Mol Physiol.* 2016;310:L824–L836.
34. Bell RE, Shaw TJ. Keloid tissue analysis discredits a role for myofibroblasts in disease pathogenesis. *Wound Repair Regen.* 2021;29:637–641.
35. Limandjaja GC, Niessen FB, Scheper RJ, et al. The keloid disorder: heterogeneity, histopathology, mechanisms and models. *Front Cell Biol.* 2020;8:360.
36. Nangole FW, Agak GW. Keloid pathophysiology: fibroblast or inflammatory disorders? *JPRAS Open.* 2019;22:44–54.
37. Wang C, Rong Y-H, Ning F-G, et al. The content and ratio of type I and III collagen in skin differ with age and injury. *Afr J Biotechnol.* 2011;10:2523–2529.
38. Jiao H, Tiran Z, Jincai F, et al. The superficial dermis may initiate keloid formation: histological analysis of the keloid dermis at different depths. *Front Physiol.* 2017;8:885.
39. da Silva IR, Tiveron LCRDC, da Silva MV, et al. In situ cytokine expression and morphometric evaluation of total collagen and collagens type I and type III in keloid scars. *Mediators Inflamm.* May 30;2017:6573802.
40. Jumper N, Hodgkinson T, Paus R, et al. Site-specific gene expression profiling as a novel strategy for unravelling keloid disease pathobiology. *PLoS One.* 2017;12:e0172955.
41. Manon-Jensen T, Karsdal MA. Chapter 14 – Type XIV Collagen. In Karsdal MA, (ed.), *Biochemistry of Collagens, Laminins and Elastin. Amsterdam: Elsevier:* 2016:93–95.
42. Dohi T, Jagannath P, Akaishi S, et al. The interplay of mechanical stress, strain, and stiffness at the keloid periphery correlates with increased caveolin-1/rock signaling and scar progression. *Plast Reconstr Surg.* 2019;144:58e–67e.
43. Naitoh M, Kubota H, Ikeda M, et al. Gene expression in human keloids is altered from dermal to chondrocytic andosteogenic llineage. *Genes Cells.* 2005;10:1081–1091.
44. Sylvie R-B, Georges B, Nathalie T. Molecular and tissue alterations of collagens in fibrosis. *Matrix Biol.* 2018;68-69:122–149.
45. Jennifer EN, Erik RO, Xiaojin Z, et al. Type VI collagen induces cardiac myofibroblast differentiation: inplications for postinfarction remodeling. *Am J Physiol Heart Circ Physiol.* 2006;290:H323–H330.
46. Silvia C, Martina C, Matilde C, et al. Extracellular collagen VI has prosurvival and autophagy instructive properties in mouse fibroblasts. *Front Physiol.* 2018;9:1129.
47. Sun S, Karsdal MA. Type VI Collagen. In Karsdal MA, (ed.), *Biochemistry of Collagens, Laminins and Elastin.* Amsterdam: Elsevier: 2016:49–55.
48. George SK, Constantina P, Ioannis P, et al. Proteomic signatures of the desmoplastic invasion front reveal collagen type XII as a marker of myofibroblastic differentiation during colorectal cancer metastasis. *Oncotarget.* 2012;3:267–285.
49. Supp DM. Animal Models for Studies of Keloid Scarring. *Adv Wound Care (New Rocelle).* 2019;8:77–89.
50. Huang C, Ogawa R. Systemic factors that shape cutaneous pathological scarring. *FASEB J.* 2020;34:13171–13184.